

The morphological evolution of the Sciara del Fuoco since 1868: reconstructing the effusive activity at Stromboli volcano

Maria Marsella · P. Baldi · M. Coltelli · M. Fabris

Received: 1 June 2010 / Accepted: 8 June 2011 / Published online: 7 August 2011
© Springer-Verlag 2011

Abstract The morphological evolution of the Sciara del Fuoco, Stromboli, is described from a time series dataset formed by Digital Elevation Models and orthophotos derived by digitising historical contour maps compiled in 1868 and 1937 and by processing data from aerial surveys carried out between 1954 and 2009. All maps were co-registered in the same reference system and used to build a quantitative reconstruction of the morphological changes of the Sciara del Fuoco slope. The changes mainly relate to the emplacement of many lava flows and their successive erosion. A comparative quantitative analysis yields estimates of areas and volumes of the lava fields formed on the sub-aerial part of the Sciara del Fuoco during a number of effusive events between 1937 and 2001, some of them never assessed before. The results of the analysis constrain the interpretation of the evolution and the magnitude of the recent effusive activity at the Stromboli volcano. Despite some uncertainties due to widely spaced observation

periods, the results integrate all available topographic knowledge and contribute to an understanding of the main characteristics of the recent effusive eruptive styles at Stromboli volcano.

Keywords Stromboli volcano · Lava flow eruptions · Digital Elevation Models · Sciara del Fuoco

Introduction

The island of Stromboli is the emerged part of an active volcano belonging to the Aeolian volcanic arc in the South Tyrrhenian Sea (Fig. 1). The volcanic edifice rises from a depth of about 2,000 m b.s.l. and reaches an elevation of 924 m a.s.l. It is the result of constructive cone-forming volcanic activity alternating with destructive lateral collapse events, the most recent of which occurred less than 5,000 years ago and formed the Sciara del Fuoco slope (Pasquaré et al. 1993; Tibaldi 2001). The Sciara del Fuoco depression is situated on the north-western flank of the volcano. It is characterized by a steep slope (up to 38°) and extends offshore to 700 m b.s.l. (Kokelaar and Romagnoli 1995).

Volcanism on Stromboli is characterized by exceptionally persistent activity over the past 1,000–1,500 years (Rosi et al. 2000). This activity consists of short, intermittent, gas-driven explosions and brief, periodic, pulsating lava fountains that take place at different craters located approximately 750 m a.s.l. in the middle–upper part of the Sciara del Fuoco. Normal activity is periodically interrupted by lava effusion and highly energetic explosions (paroxysms). The Sciara del Fuoco collects most of the scoriae, bombs, ash and blocks produced by the explosions, and it then funnels them into the sea. Furthermore, the position of the main effusive vents

Editorial responsibility: B. van Wyk de Vries

M. Marsella (✉)
Dip. Ingegneria Civile, Edile, Ambientale, Univ. “La Sapienza”,
Rome, Italy
e-mail: maria.marsella@uniroma1.it

P. Baldi
Settore Geofisica, Dip. Fisica, University of Bologna,
Bologna, Italy

M. Coltelli
Istituto Nazionale di Geofisica e Vulcanologia,
Osservatorio Etneo,
Catania, Italy

M. Fabris
Dip. Architettura, Urbanistica e Rilevamento,
University of Padova,
Padova, Italy

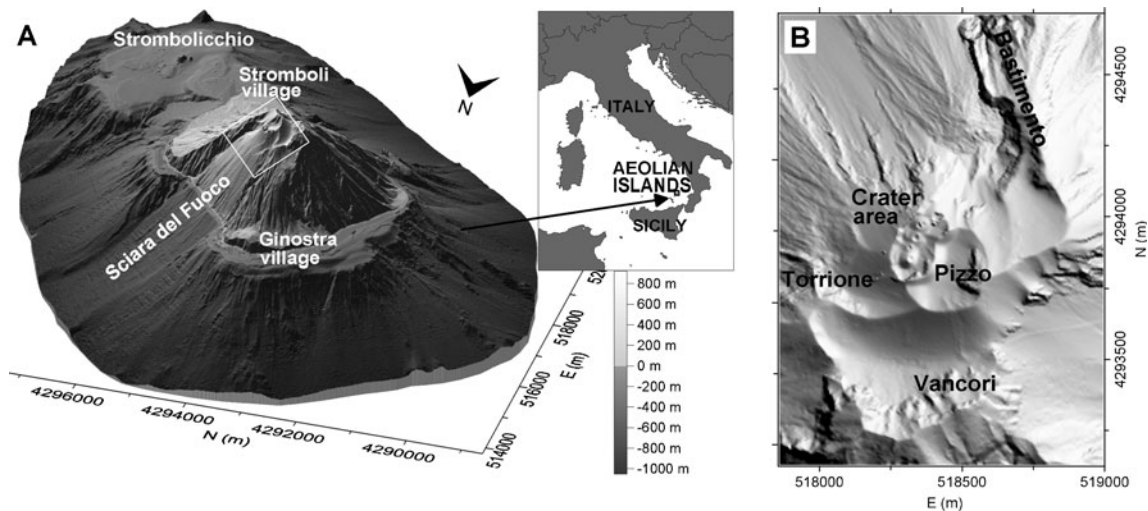


Fig. 1 a Shaded relief map of Stromboli Volcano showing the main morphological characteristics of the island, the location of the Aeolian Islands (inset) and the principal morphological features which border the Sciara del Fuoco slope (b)

inside and outside the crater area along with the morphology of the surrounding elements (Fig. 1) determines where the lava flows preferentially accumulate on the slope. Most of the lava paths have been documented for the effusive eruptions over the last two centuries.

The slope is continuously remodelled by ejecta and lava-flow deposition. It is also remodelled by erosion processes, which appear to be more substantial along the steepest portions of the slope and along the shoreline (as a consequence of the sea's action). Episodes of slope instability are not clearly reported in historical documents, but tsunamis, which in some cases affected the entire southern Tyrrhenian coast (Tinti et al. 2005), have been recently linked to landslides generated on the sub-aerial and/or the submarine part of the slope (Tommasi et al. 2005).

The most recent eruptions, which occurred in 2002–2003 and in 2007, enabled direct observations of the close connection between effusive eruptions and instability phenomena along the Sciara del Fuoco slope. Quantitative analyses were conducted to accurately estimate the geometry and the volume of the lava fields as well as of the landslide bodies. These analyses were based upon intense surveying activity conducted prior to, during and after the eruptions (Baldi et al. 2005; Marsella et al. 2009). Such knowledge has been used as a benchmark for the analyses conducted in this study, which aims at processing historical topographic maps and archived photogrammetric data to reconstruct some of the major eruptions that have occurred on Stromboli in the recent past.

More recently collected data (between 2001 and 2009) permitted a very accurate quantification of the Sciara del Fuoco's morphological evolution due to lava flow eruptions and proved that the slope evolves principally by means of

alternating constructive and destructive phases. Construction results from lava-flow emplacement along the slope during episodic effusive eruptions and from pyroclastic products continuously deposited mainly on the upper portion of the slope, near the crater area. Mass wasting is rarely linked to landslides following dike intrusions, which trigger tsunami waves; it is primarily linked to the effect of progressive erosive processes, which are more intense along the coastline than along the slope.

Recent Stromboli history indicates that the most frequent eruptive phenomena are explosive events often accompanied by short-lived lava flows resulting from overflow from the crater area. A few cases of major effusive eruptions (e.g. 1954, 1967 and 1985) are described in the literature, but the lack of direct information and quantitative data on these events prevent estimation of their magnitude in terms of the volume of erupted lava and/or the average effusion rates. It was also impossible to define the geometry of the lava fields for these events. In contrast, the last two eruptions, which occurred in 2002–2003 and in 2007, are well described by the quantitative data collected before, during and after the events. At the beginning, both events emitted large lava volumes at relatively high effusion rates; however, the two are considerably different in duration and evolution, which are both indicators of different lava effusion mechanisms (Proietti et al. 2008).

In this work, the analysis of historical data enabled a mass-balance analysis on changes in the Sciara del Fuoco surface resulting from eruptive and erosive processes between 1868 and 2001. Furthermore, a quantitative evaluation of the lava fields (i.e. determination of their area and volume of the lava accumulated on the sub-aerial part of the Sciara del Fuoco) is done on a number of effusive eruptions occurring between 1937 and 2001. This

evaluation was possible due to a comparative analysis between Digital Elevation Models (DEMs) and orthophotos extracted from aerial photostereo pairs available since 1954 as well as due to the large-scale contour-line map obtained from one of the first photogrammetric surveys performed in 1937 (Magnani 1939). The results of this analysis permitted a more detailed reconstruction of the effusive activity at the Stromboli volcano and provided useful information for investigating different discharge mechanisms.

Available data

The multi-temporal dataset adopted in our analysis is listed in Table 1 together with the main characteristics of the collected data. In addition to the photogrammetric dataset that was processed for our analysis, a detailed contour map was compiled at 1:5000 scale (Magnani 1939) by using a Santoni stereo comparator (Gruner 1977) to analyse aerial photos acquired in 1937. Also, a contour line map produced from a ground survey performed in 1868 was examined even though it should be considered of low quality. The photogrammetric images from 1954 to 1974 were selected from the Istituto Geografico Militare Italiano (IGMI) archive, and the images taken in 1992 were acquired from the Compagnia Generale Ripresearee (CGR) that generated standard mapping products. The 2001 aerial pictures were obtained by the authors during research projects dedicated to studying active volcanic areas in Italy and funded by the National Group of Volcanology (GNV). The 2001 survey covers the entire island with the aim of obtaining high-resolution maps for a project devoted to volcano monitoring. In 2001, the surface of the Sciara del Fuoco was modelled only by the erosion and deposition processes acting on the slope after a long period without

large effusive eruptions (since 1985). Therefore, the 2001 DEM was adopted as a reference dataset not solely to analyse modifications of the slope caused by the succeeding two eruptions but also to perform a back-analysis using the historical data.

Finally, images and data from between 2003 and 2009 were also collected by the authors within the frame of activities supported by the Department of Civil Protection (DPC) for monitoring the Stromboli volcano during and after the 2002–2003 and 2007 eruptions.

The scale of the aerial photos varied from 1:5,000 to 1:35,000 and the digitised images, obtained using a Wehrli Raster Master RM2 photogrammetric scanner, provided ground pixel dimensions ranging from 13 to 42 cm (Table 1). The stereo models were processed using a DPW 770 Helava Digital Photogrammetric Workstation (Socet Set software), which applied an automatic image matching procedure (Kraus 1998) to obtain a 5-m grid DEM and digital orthophotos with a pixel resolution of 0.5 m. In areas characterized by low correlation between corresponding pixels (e.g. areas with steep slopes or vegetation), a manual editing procedure was conducted to eliminate outliers and to reduce systematic effects. Manual editing also reduced the spatial gaps in the automatically extracted surface. In some cases, the DEM extraction was not possible on the entire area of interest because visibility was limited by the presence of water vapour plumes or fine ash clouds. The most recent surveys conducted for the Dipartimento Protezione Civile in 2006, 2007 and 2009 were performed using Airborne Laser Scanning sensors that provided 3D point clouds with a density of about 2 to 3 points/m². The 2006 and 2007 surveys provided the datasets employed to map and quantify the modifications of the Sciara del Fuoco slope after the 2007 eruption; the

Table 1 Principal characteristics of the datasets adopted for the time series analysis (1937–2007).

Data	23 Oct. 1937	29 Oct. 1954	20 May 1967	21 Sept. 1974	12 Nov. 1992	29 May 2001	26 July 2003	22 July 2006	23 May 2007
Mean scale	1:16,000	1:35,000	1:27,000	1:30,000	1:25,000	1:5,000	1:7,000	–	–
Characteristics	b/w	b/w	b/w	b/w	b/w	Colour	b/w	ALS	ALS
Sciara del Fuoco coverage	Complete	Partial	Complete	Partial	Partial	Complete	Complete		
Ground resolution (m)	–	0.42	0.31	0.37	0.31	0.13	0.17	0.3	0.5
Expected vertical Accuracy (m)	2.5 ^a	0.28	0.22	0.24	0.20	0.05	0.07	0.20	0.20
DEM grid s(m)	10	5	5	5	5	5	5	5	5
GPC/TIE East	–	0.80 ^b	0.17	0.19	0.16	0.03	0.05	–	–
Stand.dev. North	–	0.89 ^b	0.17	0.16	0.15	0.03	0.05	–	–
(m) h	–	0.66 ^b	0.12	0.07	0.07	0.04	0.03	–	–

^a Obtained after a residual analysis of the 1937–2001 DEM on stable areas

^b After application of a camera auto-calibration procedure

2009 survey was used to update the digital maps on the whole island and to support the detection of slope instabilities along the slope and minor failures along the coastlines.

The accuracy of the available data used to generate the multi-temporal DEMs is indicated in Table 1. The vertical accuracy of the 1937 contour-line map was assumed to be approximately 2 to 3 m. For the 1954–2003 photogrammetric datasets, the accuracy was derived from an empirical law (Kraus 1998) that provides values ranging from 0.5 to 0.05 m, assuming a horizontal accuracy equal to 1/5 of the pixel size. For Airborne Laser Scanning datasets, the accuracy was assumed to be about 0.2 m following literature data (Maas 2003).

Data processing

The 1868 and 1937 maps (Fig. 2a, b) were obtained from the IGMI archive, digitised and then processed for the extraction of vector data. In order to preserve the main relief forms, we digitised the contour lines at intervals of the same order of the expected vertical accuracy of the maps that is 10 and 5 m for 1868 and 1937, respectively. The vector data were co-registered with the photogrammetric data by using matching procedures (Pilgrim 1996; Gruen and Akca 2005). The extracted contour lines were checked via a comparative analysis with those measured using the 2001 photogrammetric data (Fig. 2c). For the 1868 maps, a preliminary planimetric co-registration was obtained using a number of corresponding points that were recognisable on both maps. Next, some digitised contour lines were compared to the corresponding curves interpolated from the 2001 DEM. A 2D affine transformation was computed and applied by adopting a least-square two-dimensional curve matching procedure (Gruen and Akca 2005) that improved the co-registration and that reduced the distance between points along the curves. By excluding the parts of the contour line curves along the slope, where significant variations were expected, a statistical analysis of the estimated horizontal discrepancies between the 1868 and the 2001 contour lines provided a null mean and a standard deviation of 20 m. When accounting for the mean slope angle of the volcanic edifice (about 30°), the vertical accuracy was estimated to be approximately 12 m. This value agrees well with the expected accuracy and includes the uncertainties due to the quality of the original map, the errors in the digitalisation process and the presence of real surface modification. To attempt a quantitative analysis of the 1868 data, we extrapolated a rough digital model of the Sciara del Fuoco area from the digitised contour lines using a grid space of 10 m.

The comparison of the contour lines from 1937 with those from the 2001 model provided a null mean and a

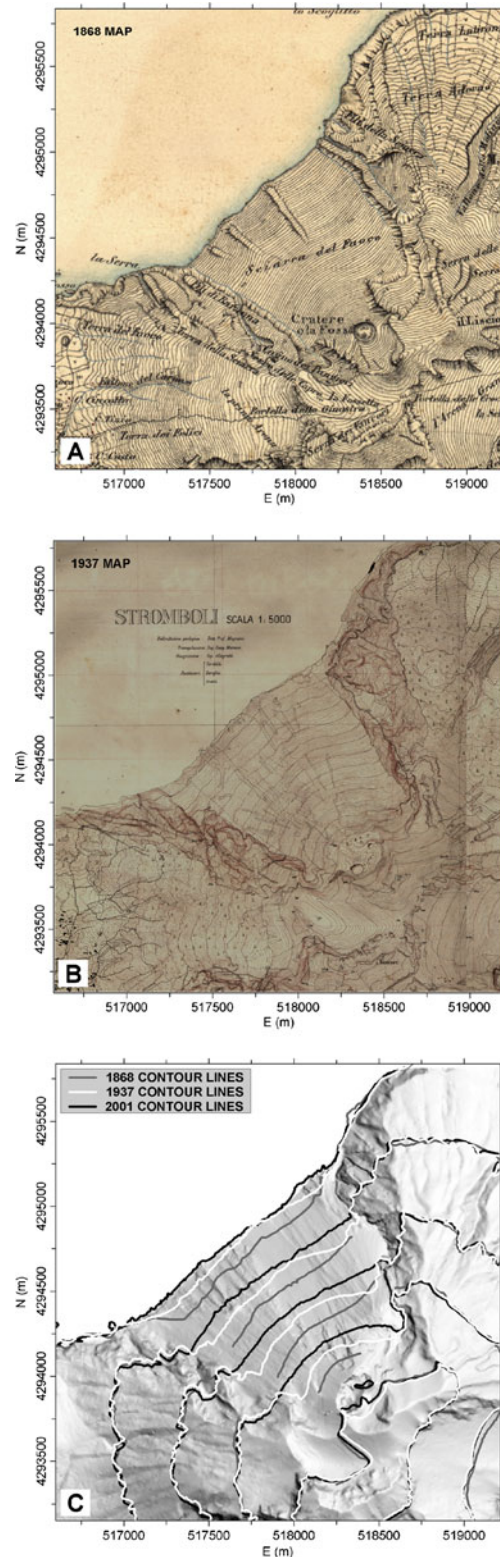


Fig. 2 The Sciara del Fuoco area as represented in **a** the 1868 and **b** 1937 topographical map from IGMI: contour lines at 200 m of interdistance are compared to those extracted from the 2001 dataset to highlight the topographical changes (**c**). The remarkable differences visible inside the Sciara del Fuoco depression are interpreted as the effect of lava flow emplacement. On the contrary, the contour lines appear in very good agreement outside of the slope

standard deviation of 9 m, and the vertical accuracy was about 5 m. All of the contour lines on the 1937 map were digitised to extract vector data for further numerical analysis. The quality and the inter-distance of the lines on this map were sufficient to generate an interpolated DEM with a grid space of 5 m. The georeferentiation of this DEM was improved through a surface-matching procedure that used the 2001 model as reference. The alignment of the two datasets was obtained by comparing data from the areas that were assumed to be insignificantly modified (i.e. the areas outside of the Sciara del Fuoco depression). The matching was performed using the Iterative Closest Point algorithm, which computes the transformation parameters (Besl and McKay 1992; Bergevin et al. 1996) necessary to minimise the distance between the two surfaces. This procedure reduced the standard deviation of the vertical residual distribution from an initial value of 5 to 2.5 m (Table 1).

The photogrammetric data was processed in a common reference system established by a Ground Control Point (GCP) network measured in 2001 with GPS. The same points were adopted for the external orientation of the 2001 images by means of a rigorous least-square aerial triangulation adjustment. To transfer the same reference system to the other photogrammetric datasets, a number of natural points, identified on stable areas (i.e. the corners of buildings and rock outcrops) were measured on the 2001 stereo models. These points were then adopted as GCPs for the aerial triangulation of all the other photogrammetric blocks. The residuals on control and tie points after the adjustments, which characterize the internal accuracy of the models, are reported in Table 1.

After the DEM extractions, a quality check on the co-registration procedure was performed via a vertical residual analysis performed using stable areas chosen on two subsequent models. The stable areas were selected on the basis of good visibility conditions, smooth morphology and absence of vegetation. After eliminating gross errors (about 5% of the data corresponding to residuals greater than 10 m) and verifying that the residual distributions did not show any systematic effects, their standard deviations ranged from 2.2 to 0.4 m (Table 2), remarkably improving for the most recent datasets. The difference between these values and the expected ones (σ_z in Table 1) is justified by the roughness and steepness of the surface.

The laser data were georeferenced by means of an integrated GPS-Inertial Navigation System that was connected to the same GPS reference station used to constrain the 2001 GCP network. As already mentioned, the 2001 DEM was often taken as a reference for the most recent morphology of the slope, modelled as reflecting only the erosive processes at lower elevations

and by explosive product deposition at the top. DEMs with a grid size of 1 m were extracted from the laser point clouds. Comparing the laser DEMs led to standard deviations of 0.3 m for the vertical residuals on stable areas (Table 2).

Differencing subsequent DEMs, an overall estimate of the volumes of the material accumulated on the sub-aerial slope or removed from it was obtained and included in Table 2. Of course, these values should be considered underestimates for those datasets that did not provide complete coverage on the slope and for those lava flows which propagated along the submarine part of the slope. By using the average standard deviations obtained for the vertical residuals, an estimate of the error associated to the volume estimates was computed through an error propagation law.

Multi-temporal quantitative analysis

To exploit the morphological and topographical comparative analysis and to attempt the identification of specific eruptions, we compiled a list of the documented effusive eruptions observed on Stromboli from 1930 to 2007 (Table 3). The information listed in the table was taken from available historical reports and from scientific papers integrating the catalogue of Barberi et al. (1993). Duration of events and the location of the vents and lava flows on the Sciara del Fuoco are also reported. The examined eruptions were subdivided into time intervals delimited by the days in which the aerial photogrammetric surveys were conducted.

The analysis was primarily based on the interpretation of Sciara del Fuoco surface modifications detected by comparison of historical maps, DEMs and orthophotos. Following the description of the various effusive eruptions in the literature, we attempted to delimitate the lava fields and to quantify the emitted lava volumes by using a GIS tool to process the whole dataset. Considering the lack of precise historical information, the lacunae in the topographical data and the overlap of lava fields from different eruptions, in some cases only a semi-quantitative lava field reconstruction was possible. A summary of the results obtained by our quantitative analysis is shown in Table 4 and in Fig. 3, while a more detailed description of how the different eruptions were identified is illustrated in the following paragraphs. In particular, it should be underlined that for a few eruptions the estimated lava volumes and associated rates are underestimated because the lava flow affected also the submarine portion of the slope.

Comparison of the 1868 and 1937 historical maps

Historical sources document many lava flow eruptions (more than 30 episodes), at least one landslide and three

Table 2 Results from the comparative time series DEM analysis

	Compared data	Mean Vertical Residuals (m)	Volumes (10^6 m^3)	
			Accumulated	Eroded
Mean and standard deviation of vertical residual computed in area not involved in deformation and/or lava flow emplacement and overall estimates of accumulated and eroded volumes and their associated errors. These values should be considered underestimated for those dataset that did not provide complete coverage on the Sciara del Fuoco	1937–1954	-0.3 ± 2.2	46.3 ± 2.8	0.6 ± 0.2
	1954–1967	-0.5 ± 1.2	8.7 ± 1.0	2.1 ± 0.7
	1967–1974	-0.2 ± 0.9	1.0 ± 0.3	2.1 ± 0.4
	1974–1992	0.2 ± 1.0	1.4 ± 0.1	4.6 ± 0.6
	1992–2001	-0.2 ± 0.6	1.1 ± 0.1	0.9 ± 0.1
	2001–2003	0.0 ± 0.4	2.8 ± 0.2	6.6 ± 0.3
	2003–2006	0.1 ± 0.4	0.1 ± 0.1	2.1 ± 0.1
	2006–2007	-0.1 ± 0.3	4.6 ± 0.2	4.5 ± 0.3

tsunami waves that occurred between 1868 and 1937 (Barberi et al. 1993). The maps in Fig. 2 show that in this time interval, the Sciara del Fuoco depression was significantly filled. By comparing the 1868 and the 1937 surface obtained interpolating the digitised contour lines, a total volume of about $50 \times 10^6 \text{ m}^3$ was estimated to have accumulated along the slope. This figure appears justified by the high number of documented lava flows.

In the last few years of this period a major event, the eruption of 1930 that formed lava flows, hot avalanches and tsunami waves, was described in detail by Rittmann (1931), Imbo' (1933) and Abruzzese (1935). For this period through 1937, our reconstruction (Table 3) indicated about 180 days of continuous or intermittent lava flow episodes. In 1937, the contiguous effusive episodes recorded between 6 January and 24 September may be interpreted as being the effect of one long-lasting eruption.

Analysis of the 1937 DEM and of the corresponding aerial images (Fig. 4) highlights some interesting features linked to the volcanic activity: partially eroded lava deltas (ld) are clearly visible along the coastline and are the effects of the eruptions that were often characterized by “impressive lava flows reaching the sea” (Abruzzese 1937; 1940); the depressed area (dd) on the Sciara del Fuoco's north-eastern side cannot be directly linked to documented slope failures and may be relics of the scar visible in 1868 or the effect of a more important growth of the adjacent area (on the central–western side of the slope) where lava may have preferentially accumulated; on the south-western side on the slope, a small scar (s) is visible at about 700 m a.s.l., and it is enclosed within a wide slightly depressed area (wd). The scar is very likely the effect of a vent opening that produced a lava flow that reached the sea and formed the delta still partially visible along the shoreline. In the upper-south-western portion, overlapped lava fields, reported many times between 1935 and 1937, are clearly visible and marked by morphologic features. Such features completely disappeared in the following years.

Sciara del Fuoco changes observed between 1937 and 2001

Historical records indicate that between 1937 and 1954, several lava flows and a tsunami occurred. The latter occurred on 20 August 1944 and was described by Cavallaro (1957a, b). Major effusive activity was observed in 1938–1939, with lava flows reaching the sea and emplaced upon the whole slope. In 1941, two flows occurred on the south-western side of slope and the period between 1943 and 1944 was characterized by intermittent lava flows along the south-western border of the slope (Abruzzese 1940; Ponte 1948; Cavallaro 1957a). In the following years, between 1945 and 1948, only moderate activity was reported; this may be because of the interruption of direct observations after World War II rather than because of an actual quiescent phase. Afterwards, constant moderate explosive activity was interrupted by short-lived effusive eruptions in 1949, 1950 and 1952, which mainly accumulated along the north-eastern sector of Sciara del Fuoco, as described by Bullard (1954), Cucuzza Silvestri (1955) and Cavallaro (1957b). Finally, a major eruption started on 1 February 1954; its features were comprehensively described by Cucuzza Silvestri (1955).

Comparison of the DEMs from 1937–1954 was used to create a residual map (Fig. 5a), which shows that the slope underwent an accretion phase in this period. For this period, we estimated that a volume of $46 \times 10^6 \text{ m}^3$ of lava accumulated along the sub-aerial slope. Larger thicknesses observed in the south-western upper side may be accredited both to overlapping lava flows and to explosive product accumulation on the depressed area that corresponds to the scar (Fig. 4c) observed below the Torrione dike (indicated in Fig. 1) as visible on the 1937 DEM. It may be worth mentioning that the frequent explosive events, often referred in the historical documents as “the activity of the Torrione crater”, may have emitted products that have principally deposited on the upper western side of the slope.

To substantiate such a large growth, we compared cross sections (Fig. 6) cut between 200 and 500 m a.s.l.

Table 3 Major historical lava flow eruptions recorded at Stromboli volcano between 1868 and 2007 and date of surveys

Year	Description	Active days	Reference
1868	IGMI Map		
1868–1930	19 Lava flows, 2 tsunami waves, 1 landslide		Barberi et al. (1993)
1930	Lava flow and tsunami waves (11 Sept.), lava flows (1–2 Dec.).	~2	Rittmann (1931)
1935	Flow to the sea (25–27 Feb.)—Continuous effusion (21 Jul.–27 Aug.)	~38	Abruzzese (1937)
1936	Flow to the sea, submarine cable cut (31 Jan.)—Continuous effusion (9 Sept.–7 Oct.)	~30	Abruzzese (1937)
1937	8 contiguous episodes (6 Jan.–24 Sept.)—Impressive flow to the sea (1–20 Jun.)	110	Abruzzese (1940)
23-ott-37	<i>IGMI Survey/Map</i>		
1937	3 lava flows to the sea (14–15 Dec.)	2	Abruzzese (1940)
1938	Intermittent flows/overflows—Large flows forming fans at the coastline (11 Jan.–June)—Continuous effusion (11 Oct.–12 Nov.)	~67	Abruzzese (1940)
1939	Intermittent lava flows along the whole slope (10 Jan.–8 Jun.)	~34	Abruzzese (1940)
1941	2 flows along the SW side (22 Aug.–7 Sept.)	15	Ponte (1948)
1943	Intermittent lava flows along the SW side—Continuous effusion (3 Dec.–???)	~20	
1944	Intermittent flows on SW side (until 30 Oct.)—Lava delta, tsunami wave (20 Aug.)	~70	
1945	US Air Force Survey		USGS archive
1949	Flows along the NE side (6–?? Jun.)	~3	Cavallaro (1957a)
1950	Flows along the NE side (20–24 Oct.)	~5	Cucuzza Silvestri (1955)
1952	Flows along the NE side (7–17 Jun.)	15	
1954	Flows along the NE side (1 Feb.–13 Mar.)	42	
29 Oct 1954	<i>IGMI Survey</i>		
1954	Flows along the NE side (6–7 Dec.)	2	Cavallaro (1957b)
1955	Vent at low elevation, lava fan (28 Feb.–20 Mar.) Flow on the 1954 lava (22–23 Mar.)	24	Abruzzese and Cavallaro (1955)
1956	Intermittent flows along NE side (1 Jan.–16 Mar.)	75	Cavallaro (1957b, 1958)
1958	Lava flow forming fan along SW side (2–12 Feb.) Lava flow forming fan along NE side (31 May–5 Jun.)	11	Cavallaro (1970)
1959	Overflows (12–13 Aug.)	1	
1967	Lava eruption (19 Apr.–20 May)	31	Gasparini et al. (1967)
20 May 1967	<i>IGMI Survey</i>		
1967	Lava eruption (20 May–13 Aug.)	83	Capaldi et al. (1978)
1971	2 flows along the NW side (3 Apr. and 1 May)		www.volcano.si.edu
21 Sept. 1974	<i>IGMI Survey</i>		
1975	Lava eruption (4–24 Nov.)	20	Capaldi et al. (1978) Nappi (1976)
1985–1986	Lava eruption (6 Dec. 1985–26 Apr. 1986)	145	De Fino et al (1988)
12 Nov. 1992	<i>Photogrammetric Survey</i>		CGR
1993	Overflows on the NE side (16 and 18 May)	~1	
29 May 2001	<i>Photogrammetric Survey</i>		GNV
2002–2003	Lava eruption, 1 landslide, 1 tsunami (28 Dec. 2002–22 Jul. 2003)	207	Baldi et al. (2005)
27-ago-03	<i>Photogrammetric Survey</i>		GNV/DPC
22 July 2006	<i>ALS Survey</i>		DPC
2007	Lava eruption (28 Feb.–12 Apr.)	35	Marsella et al. (2009)
22 May 2007	<i>ALS Survey</i>		DPC

parallel to the shoreline on the 1937, 1954 and 2001 surfaces. First, the good agreement outside the Sciarra del

Fuoco depression demonstrated the absence of systematic errors. On the other hand, the sections also indicated that

Table 4 Summary of the results from the single eruption quantitative analysis containing for each considered eruption

Eruption	Sciara del Fuoco sector	Duration (days)	Lava field area (10^5 m^2)	Estimated eruption rate (m^3/s)	Estimated lava volume (10^6 m^3)
<i>1937</i>	All	2			0.2 ^a
<i>1938</i>	All	67		1.0	5.6
<i>1939</i>	All	34			2.8
<i>1941</i>	SW	15			3.0
<i>1943</i>	SW	20	4.2	2.3	3.9
<i>1944</i>	SW	70			13.8
<i>1949</i>	NE	3			1.0
<i>1950</i>	NE (?)	5	1.7	3.9	1.7
<i>1952</i>	NE	15			5.0
<i>1954</i>	NE	42	1.5	1.3	4.8
<i>1954</i>	NE	2			0.1
<i>1955</i>	NE	2			0.1
<i>1956</i>	NE	75	3.2	0.5	3.2
<i>1958</i>	NE	4			0.2
<i>1958</i>	SW	7	1.3	0.7	0.4
<i>1959</i>	Overflows	–	1.1	–	1.1
<i>1967</i>	SW	114	2.5	0.7	6.8
<i>1975</i>	Central	20	0.3	0.1	0.1
<i>1985^b</i>	NE	145	2.6	0.3	3.3
<i>1993</i>	NE				0.1
<i>2002–2003</i>	NE	207	3.2	0.7	12.5
<i>2007</i>	NE	35	3.2	3.5	10.6

The year and the duration of the activity derived from historical records; the lava field area and the volume of the lava accumulated on sub-aerial part of the Sciara del Fuoco as reconstructed from the analysis of the photogrammetric and laser datasets; an average eruption rate which in the first years was extrapolated from a cumulated value. The italicized dates refer to eruptions which affected also the submarine portion of the slope. The associated rates should be considered underestimated

^a Values extrapolated on the basis of each eruption's duration using an average effusion rate.

^b Obtained merging the 1992 DEM, available on about 1/3 of the Sciara del Fuoco slope, with the 2001

the Sciara del Fuoco depression was uniformly filled between 1937 and 1954 and produced a surface that almost coincides with that measured in 2001. These data showed that all lava flows deposited by eruptions after 1954 were either very thin or almost completely eroded afterward.

The comparison of an aerial image taken by the US Air Force in 1945 (Fig. 5b) to the 1937 and 1954 IGMI ones provides useful insights for discriminating between different eruptions. The 1945 aerial image shows that close to the western slope boundary, the coastline had retreated. This may be the artefact of a submarine slide that was presumably the cause of the tsunami that occurred on 20 August 1944 (Table 3), which affected

the surrounding islands and the Sicilian coast. This event has alternatively been attributed by Cavallaro (1957a) to a hot avalanche travelling along the “Sciara Vecchia” depression. In 1954, the slope surface was characterized by morphological elements that clearly correspond to numerous lava flows reaching the sea along the entire width of the slope. Along the western side, the area below the Torrione dike appeared to be covered by many overlapping, short-length lava flows that clearly did not reach the sea. This area may have been affected by the effusive activity described by Cavallaro (1957a, b) and Ponte (1948) for the interval between 1937 and 1944. In particular, the activity observed in 1943–1944 was characterized by long-lasting, large flows that left a very

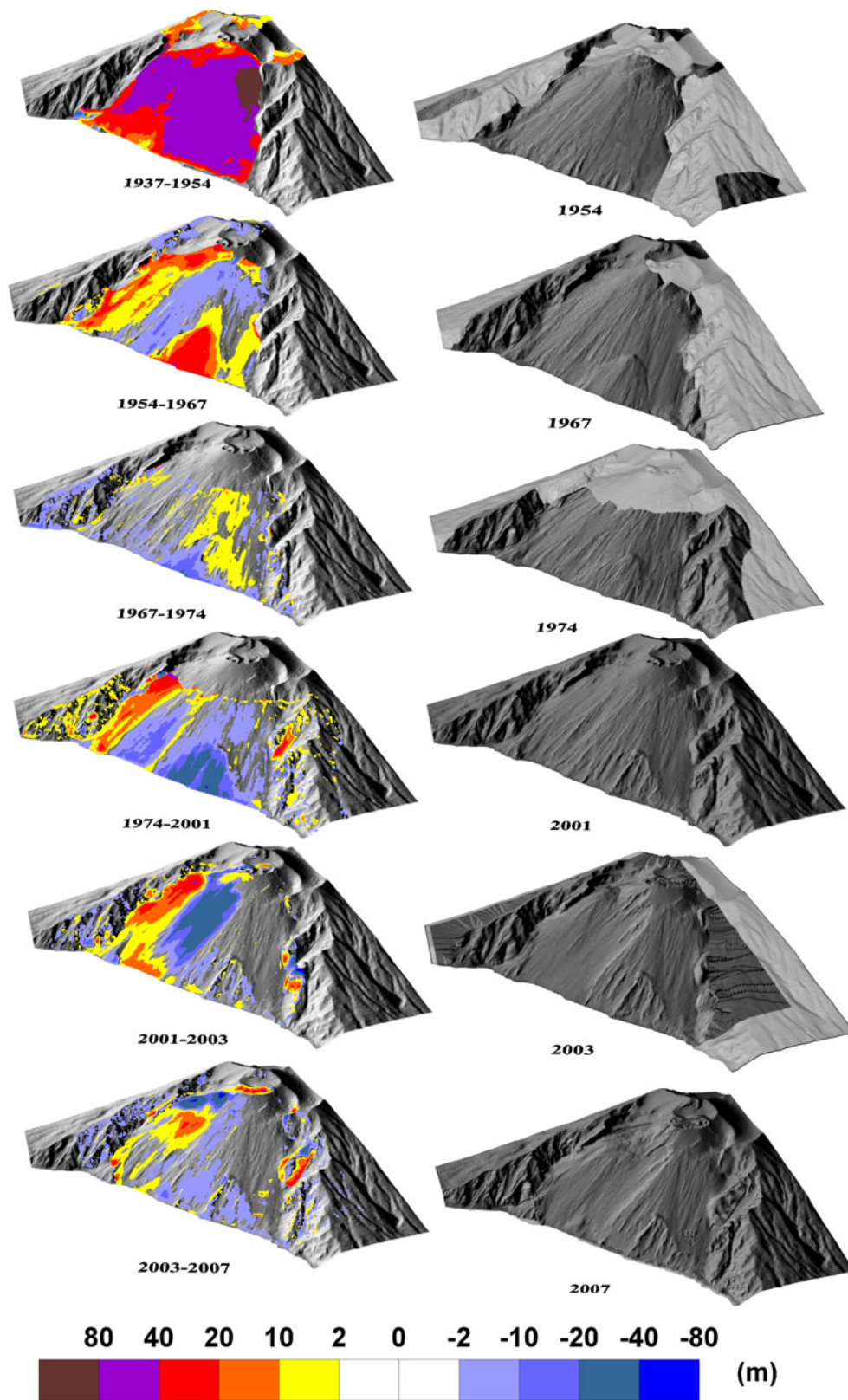
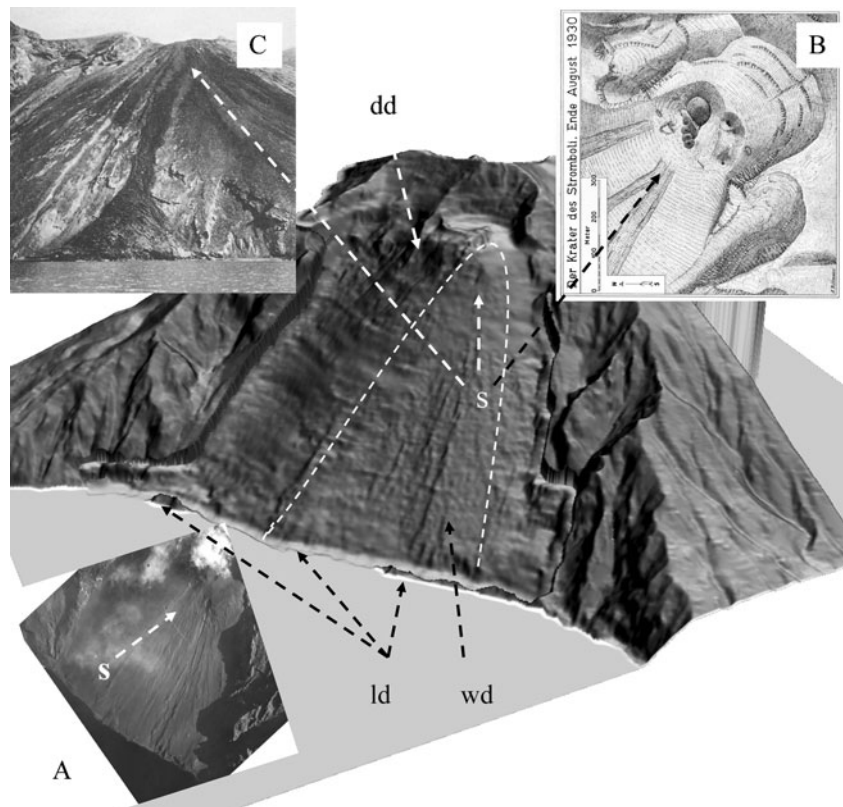


Fig. 3 Sequence of 3D views of the results from the multi-temporal analysis conducted between 1937 and 2007: on the *left*, the elevation differences (residuals) computed comparing two subsequent DEMs

draped on the Sciara del Fuoco surface; on the *right*, the *shaded* relief maps of the surface at the end of the considered period

Fig. 4 3D view of the 1937 shaded relief map compared to the IGMI 1937 aerial image (a) and sketches (b, c) of the effect of the 1930 eruption from Rittmann (1931). Features linked to the volcanic activity are indicated as follows: partially eroded *ld*, *dd*, *s*, *wd*



thick layer of lava on the south-western side of the slope. The shoreline retreat visible in the 1945 photo has disappeared due to the combined effects of the sea and the infilling process, and the debris of this process originated at the upper part of the slope. On the east side, the formation of a delta from the lava flow is evident along the shoreline and corresponds to the well-documented eruption that started in February 1954 (Cucuzza Silvestri 1955). This lava flow likely overlapped with the lava field from the eruptions that occurred in the years 1949, 1950 and 1952 (Table 3).

Using the aforementioned reconstructions, we extracted a map of lava fields for different eruptions (Fig. 5a), and we were able to estimate the corresponding lava volumes shown in Table 4. Unfortunately, the first three eruptions (1937, 1938 and 1939) cannot be positioned along the slope, and because of overlapped lava fields, the following eruptions were grouped into two periods, 1941–1944 and 1949–1952. Thus, even though only a semi-quantitative volume assessment (overestimated by about 10%) was possible, useful information into the characteristics of effusive eruptions from this period can be outlined:

1. Two large eruptions occurred in 1938 and 1939 with a volume of about 5.6×10^6 and 2.9×10^6 m³, respectively.
2. Between 1941 and 1944, lava flows invaded mostly the south-western sector of the slope, and the 1944 eruption was the largest event, with a maximum volume of $13.8 \times$

10^6 m³; the 1941 and 1943 lava volume was estimated to be about 3.0×10^6 and 3.9×10^6 m³, respectively.

3. The 1949, 1950 and 1952 lava flows, covering the north-eastern sector, had a volume of 1.0×10^6 , 1.6×10^6 and 5.0×10^6 m³, respectively.
4. The 1954 eruption was mapped and its volume (4.8×10^6 m³) estimated without considering the lava delta submarine portion of the lava delta.

In the time interval between the 1954 and 1974, a number of lava flow eruptions covered the slope and were recorded together with other less significant events, which we have identified as overflow episodes. The most relevant lava flows were emplaced in 1955, 1956 and 1967.

The analysis of the residual maps obtained by differencing the 1954 and 1967 DEMs (Fig. 5c) and of the corresponding orthophotos permitted us to delimit the different lava flows emplaced during this period (Fig. 5d). On the western side, the accumulation is attributed to the lava extrusion that occurred in 1955 at the base of the flank and was then overlapped by the 1967 eruption. The lava field visible along the south-western boundary of the slope was attributed to the eruption that occurred between 6 and 12 February 1958 (Cavallaro 1970). On the opposite side (north-east) of the slope, we identified the area affected by the lava flows reported in 1954 (6–7 December), 1955 (22 March), 1956 (1–14 January, 16 January–16 March) and 1958 (31 May–5 June). Additionally, we roughly delimited the area covered

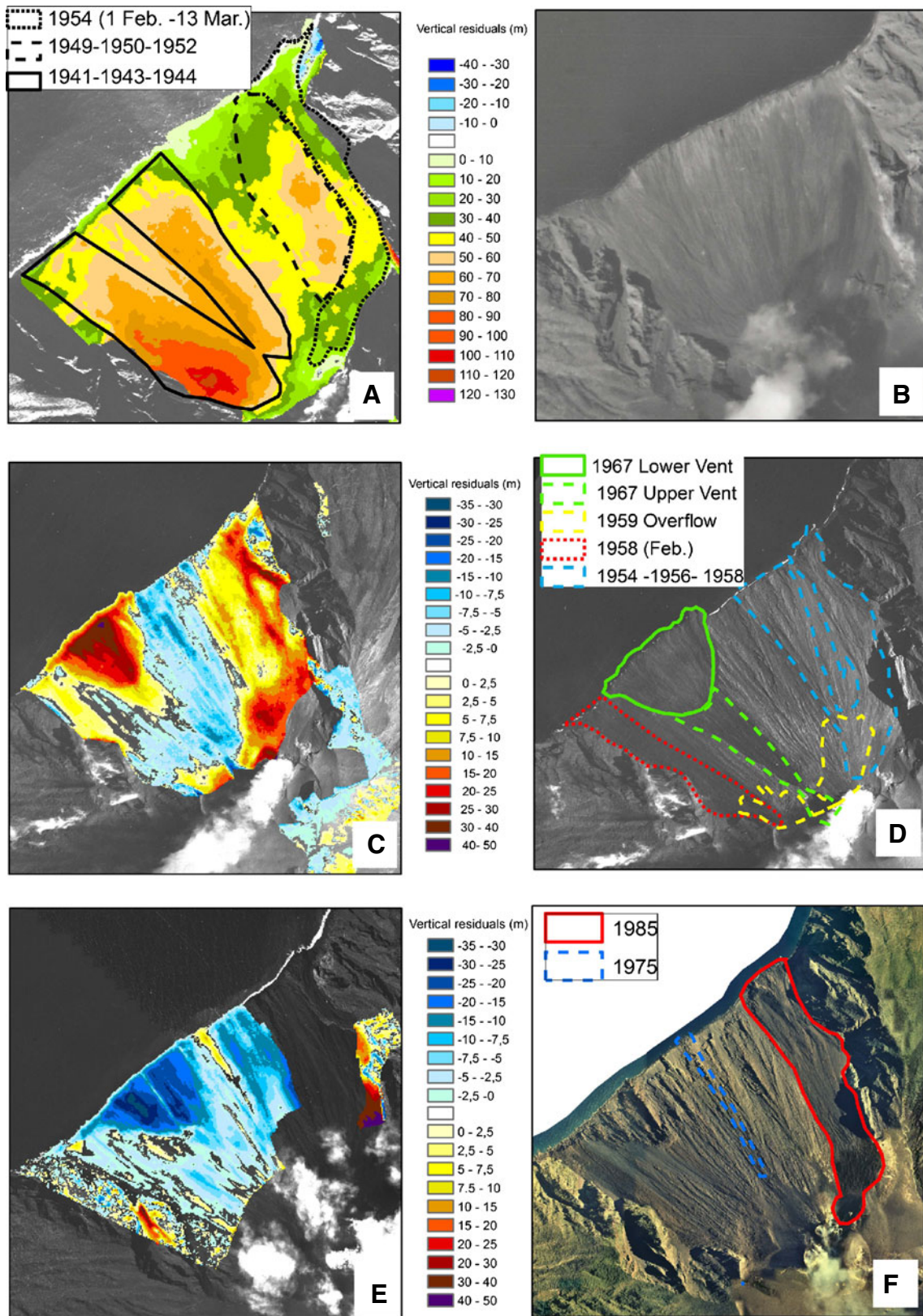


Fig. 5 Comparison between 1937 and 1954: **a** lava flow limits traced on the residual map showing the vertical difference in metres, **b** 1945 aerial image; **c** comparison between 1954 and 1967: lava flow limits were mapped out on the residual map showing the vertical difference in metres obtained differencing the 1967 and 1954 DEMs and **d** the

lava flows mapped on the 1967 orthophoto; **e** comparison between 1974 and 1992: lava flow limits were mapped out on the residual map showing the vertical difference in metres obtained differencing the 1992 and 1974 DEMs and **f** the lava flows mapped on 2001 orthophoto

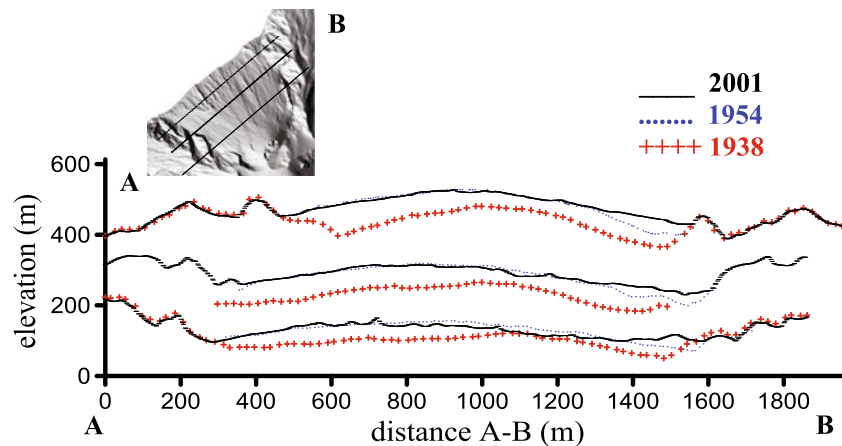


Fig. 6 Comparison of profiles cut across the Sciara del Fuoco on the 1937 (*cross symbol*), 1954 (*dotted symbol*) and 2001 (*line*) surfaces proceeding from *A* (along the SW border of the slope) to *B* (along the NE side)

by the lava produced by moderate overflows during the intense explosive activity of 1959 (Cavallaro 1970).

The 1967 eruption started on 19 April and ended on 13 August (Capaldi et al. 1978) involving the south-western sector of the slope. It was described by Gasparini et al. (1968) who used direct observation of the first days of activity. The paper includes photos that, together with the aerial images acquired on 20 May 1967, were used for defining the lava fields. The aerial image (Fig. 5d) enabled us to identify the eruptive fissure cutting the crater rim and the newly formed lava field, although no clear evidence of active flows is discernible. This clearly indicates that, on 20 May 1967, the eruption was either experiencing a period of very low effusion or was in its terminal phase.

The 1967 lava accumulated in a very large depression extending from the coastline up to about 700 m a.s.l. (Fig. 5c) and which corresponded to a volume of $4.2 \times 10^6 \text{ m}^3$ that was either eroded or collapsed. This depression almost certainly formed between 1954 and 1967, and it is most likely to be the effect of erosive processes because there are no records of large slope failure phenomena. The magnitude and the geometry of the depressed area suggest that it may be the consequence of the magma emptying process from the dyke intrusion at a very low elevation like that occurred during the 1955 effusive submarine activity, as visible in the photos in Abruzzese and Cavallaro (1955).

Table 4 indicates a volume of $3.2 \times 10^6 \text{ m}^3$ for the 1956 eruption and $6.0 \times 10^6 \text{ m}^3$ accumulated between 19 April and 20 May 1967. The latter was estimated after applying a correction to account for the effect of the depression. The volume of the 1967 lava flows is certainly underestimated because it did not include the lava emplaced below sea level, which may be significant considering the construction of such a large lava delta along the coastline. We could not account for the contribution of the 1955 eruption because it was mainly submarine (Abruzzese and Cavallaro 1955) and its sub-aerial

portion almost disappeared after about one year, as shown in a photo from Cavallaro (1958). Assuming that the observed depression was really caused by this eruption, it may also be inferred that the eruption volume may have been large.

Significant eruptions were not recorded in the period 1967–1974, with the exception of the 1967 eruption, which it is believed to have ended on 13 August, 83 days after the aerial survey was conducted. Two small lava flows were observed on 3 April and on 1 May 1971: both flows lasted only one day and flowed from the top to the sea on the NW side of the Sciara del Fuoco. The comparison of the 1967 and 1974 DEMs (Fig. 3) can only be used to observe the volume, enclosing also an eroded area in proximity of the coastline (related to the lava flows that were active from 20 May until the end of the 1967 eruption). Thus, Table 4 includes an estimate of the total volume of the 1967 eruption, obtained adding to the one estimated for the period 19 April–13 August, a volume of $0.9 \times 10^6 \text{ m}^3$ measured comparing the 1967 and 1974 DEMs. We obtained for the whole eruption an average effusion rate of $0.7 \text{ m}^3 \text{ s}^{-1}$, surely underestimated since not accounting for the lava accumulated below sea level. Furthermore, it should be noted that after 20 May the eruption was experiencing an ending phase characterized by a very low average effusion rate ($0.1 \text{ m}^3 \text{ s}^{-1}$) in respect to that estimated for the first period ($2.2 \text{ m}^3 \text{ s}^{-1}$). Consequently, the 1967 eruption was the last major event (associated to a sub-aerial volume of about $6.8 \times 10^6 \text{ m}^3$) that opened vents in the south-western sector of the slope.

Between 1974 and 1992, two major eruptions occurred: one was described by Nappi (1976) and Capaldi et al. (1978) and lasted from 4–24 November 1975, and the second one was described by De Fino et al. (1988) and was active from 6 December 1985 to 26 April 1986.

Because of clouds and plume coverage, the residual map in Fig. 5e only partially depicts the elevation changes that occurred in this period. The erosion process visible at the

foot of the slope affects the lava fan produced by the 1967 lava flow (Fig. 5e) superimposed onto the 1955 flow. The small tongue of lava visible in the central area may be attributed to the 1975 eruption. Positive residuals up to 50 m, visible along the eastern side of the slope are attributed to the 1985 lava flow. An estimation of the volume erupted during the 1975 and 1985–86 eruptions (about 0.1×10^6 and 3.3×10^6 m³, respectively) was possible by comparing the 1967 surface to the 2001 surface. From 1986 until December 2002 no effusive activity was observed apart from two small lava overflows which occurred on May 16 and 18, 1993 on the NE side of the upper slope. Thus, on the 2001 orthophoto (Fig. 5f), it was possible to trace the lava field of the 1975 and 1985 eruptions.

The 2002–2003 and 2007 eruptions

On 28 December 2002, lava started to flow along the north-western side and was soon followed by a large landslide that affected both the submarine and the sub-aerial portions of the Sciara del Fuoco and that mobilised about 30×10^6 m³ of material (Tommasi et al. 2005). Photogrammetric surveys repeated during the whole eruption allowed us to quantify the morphological evolution of the slope due to ongoing erosive and accumulation processes: a total volume of 12.5×10^6 m³ of erupted lava (Baldi et al. 2008) was estimated corresponding to an eruption rate of about 0.7 m³ s⁻¹ (Marsella et al. 2009) and a maximum effusion rate of about 13 m³ s⁻¹.

The comparison of the 2003 and 2001 DEMs (Fig. 3) showed remarkable changes of the slope resulting from the 2002–2003 eruption (Baldi et al. 2005; Marsella et al. 2008). A lava terrace was built approximately 600 m a.s.l. during the last period of the eruption, and a very large depressed area was formed by the evolution of the scar from the landslide that occurred at the eruption's onset (Tommasi et al. 2008). This long-lasting eruption left a very thick layer of lava on the north-eastern side of the slope that was similar to that produced during the 1944 activity along the south-western side. The two eruptions have many similarities. Both were emitted mostly from a main vent at about same elevation, and the lava fields have a similar geometry. Their width and thickness were similar and even if the flows reached the sea, they did not form significant fans. Each also formed a thick terrace on the top of the slope, and the main flows both lasted for many days. Strong explosions also occurred during both events' effusive activity, and both triggered a tsunami wave. The 2002–2003 eruption represented the first event that was directly observed and quantified during its whole duration, and it was useful for understanding how constructive (through lava emplacement and debris accumulation) and destructive

(through failures induced by magma intrusion and erosion) processes alternate and/or overlap.

The comparison of the 2003–2006 DEMs (Fig. 3) showed the slope's evolution relative to the overall progressive erosion of the shallower portions of the recent lava layer (from 2002–2003) that accumulated along the slope, especially along the coastline. The comparison was also examined relative to the erosion from the retrogression of the escarpments landslide that occurred on 30 December 2002. There was also a significant infilling process of the crater area.

On 27 February 2007, a new eruption started on Stromboli when a vent opened at the base of the north-eastern crater (about 600 m a.s.l.) near the lava terrace that had formed during the last phase of the 2002–2003 eruption (Fig. 7). The dike intrusion significantly rearranged the upper part of the slope, including the crater area (Fig. 7a) and caused a volumetric collapse (Fig. 3). The lowering of the surface was not associated to destructive mass failures, like those observed in 2002–2003, but appear similar to what was observed on the 1967 surface, which we have considered connected to the 1955 eruption.

A second vent opened at a lower elevation (about 400 m) and emitted a lava flow that lasted until the end of the eruption on 2 April 2007. Lava from the main vent produced a compound, fan-shaped flow field and discharged most of the lava into the sea. This discharge resulted in the creation of a very large lava delta with a width of approximately 600 m and a length of approximately 100 m, which covered the small 2003 lava fan (Fig. 7b) and was quite comparable to that formed by the 1967 eruption. During the latest eruption, three photogrammetric and two airborne laser scanner projects were conducted. The final volume emplaced on the sub-aerial slope by the main vent was 2.7×10^6 m³, whereas the total volume discharged during the 2007 eruption was estimated at 10.6×10^6 m³ (Marsella et al. 2009) and corresponded to an eruption rate of about 3.5 m³ s⁻¹. The maximum computed effusion rate value was about 4.5 m³ s⁻¹. The effects of the 2007 eruption have many similarities to those of the 1954 eruption: the lava fields are almost identical including the large fan was constructed along the coast (50 m wide and 4–10 m thick). Also, the main vent was at about 700 m a.s.l. and the vent alignment appears similar (Fig. 7c). Both events lasted about a month and emitted a similar lava volume, considering that for the 1954 event, it was only possible to estimate the volume of the sub-aerial deposit.

Discussion

The analysis of the lava flow distribution (Fig. 8a), as well the estimates of area and volume for each event (Table 4), allowed us to recognize two eruptive styles characterizing

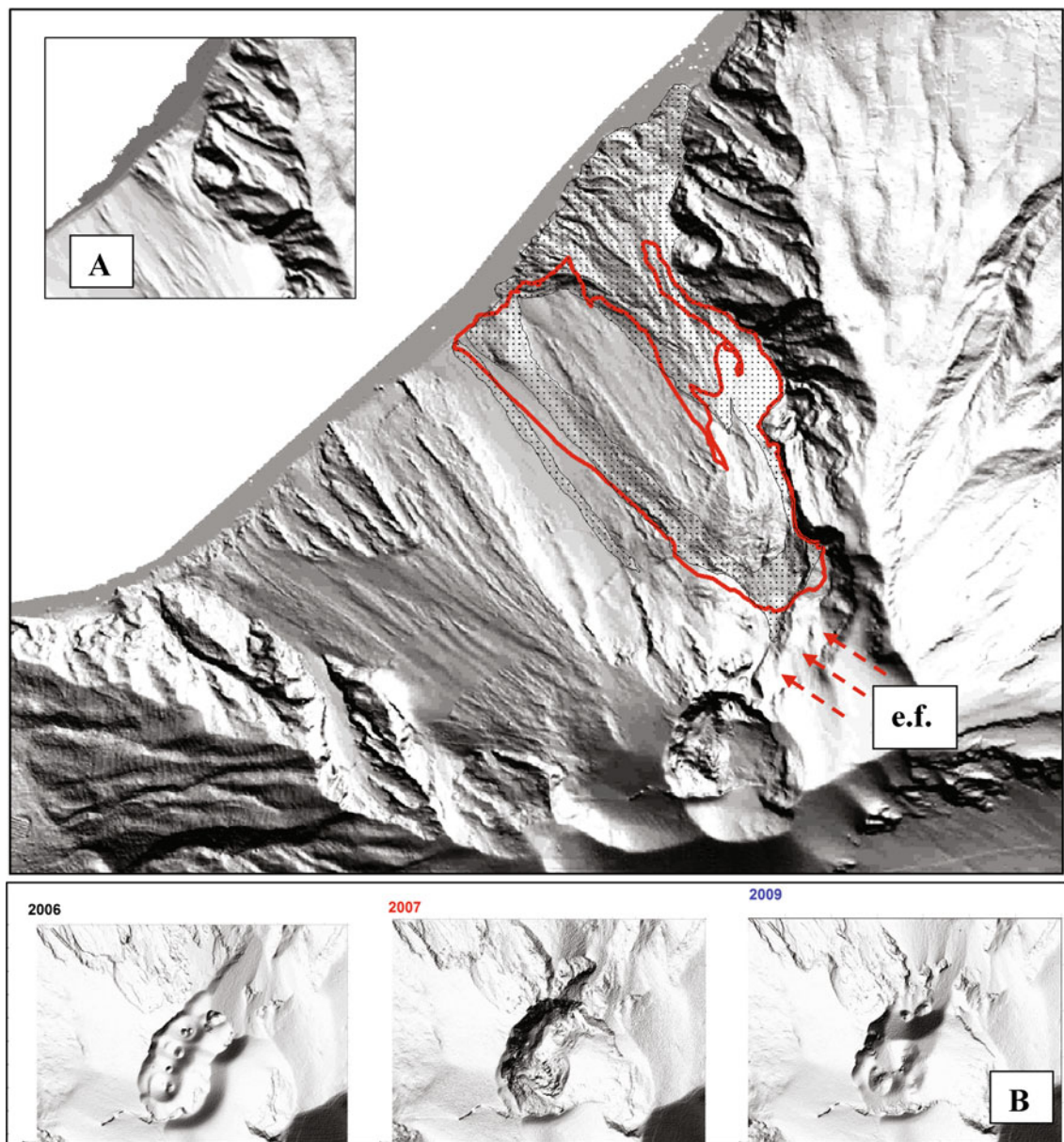


Fig. 7 Shaded relief image of the up to date Sciara del Fuoco surface (2009 laser survey) with the limits of the 2002–2003 (solid thick line) and 2007 (dotted area) lava fields; the *inset A* shows a detail of the 2003 surface where the large lava delta built up during the 2007

eruption; the *inset B* shows that in 2006 the vents inside the crater area were aligned along the same direction of the eruptive fissure (*e.f.*), and after the collapse of the internal crater sectors in 2007, a new vent formed along the same trend (2009)

the recent effusive activity at Stromboli and probably linked to different lava discharge mechanisms.

Most of the lava fields covering the north-eastern sector of the slope are formed by quite abundant lava flows often reaching the coastline and propagating below the sea, as testified by the construction of fairly large lava deltas in 1954, 1985 and 2007 (Fig. 8b). Generally, the most relevant lava flows are emitted from vents situated at the base of the crater terrace at elevations usually higher than 600 m. As directly observed during the 2002–2003 and 2007 eruptions, the vents that initiate the activity appear aligned

along the same direction. This is interpreted as being the expression of the shallower portion of the magma intrusion that should consequently mark the strike of the eruptive fissure. Also the geometry of the 1954 and 1985 lava fields appear consistent with the presence of a dike intersecting the summit vents and forming eruptive fissures similar to that observed in 2002–2003 and 2007 (Fig. 7).

As a consequence, lava emission from the north-eastern side (Fig. 8c) can be seen as the expression of a dike intrusion, which breaches the crater rim and guides the lava flows along the lateral slope escarpments. Depending on

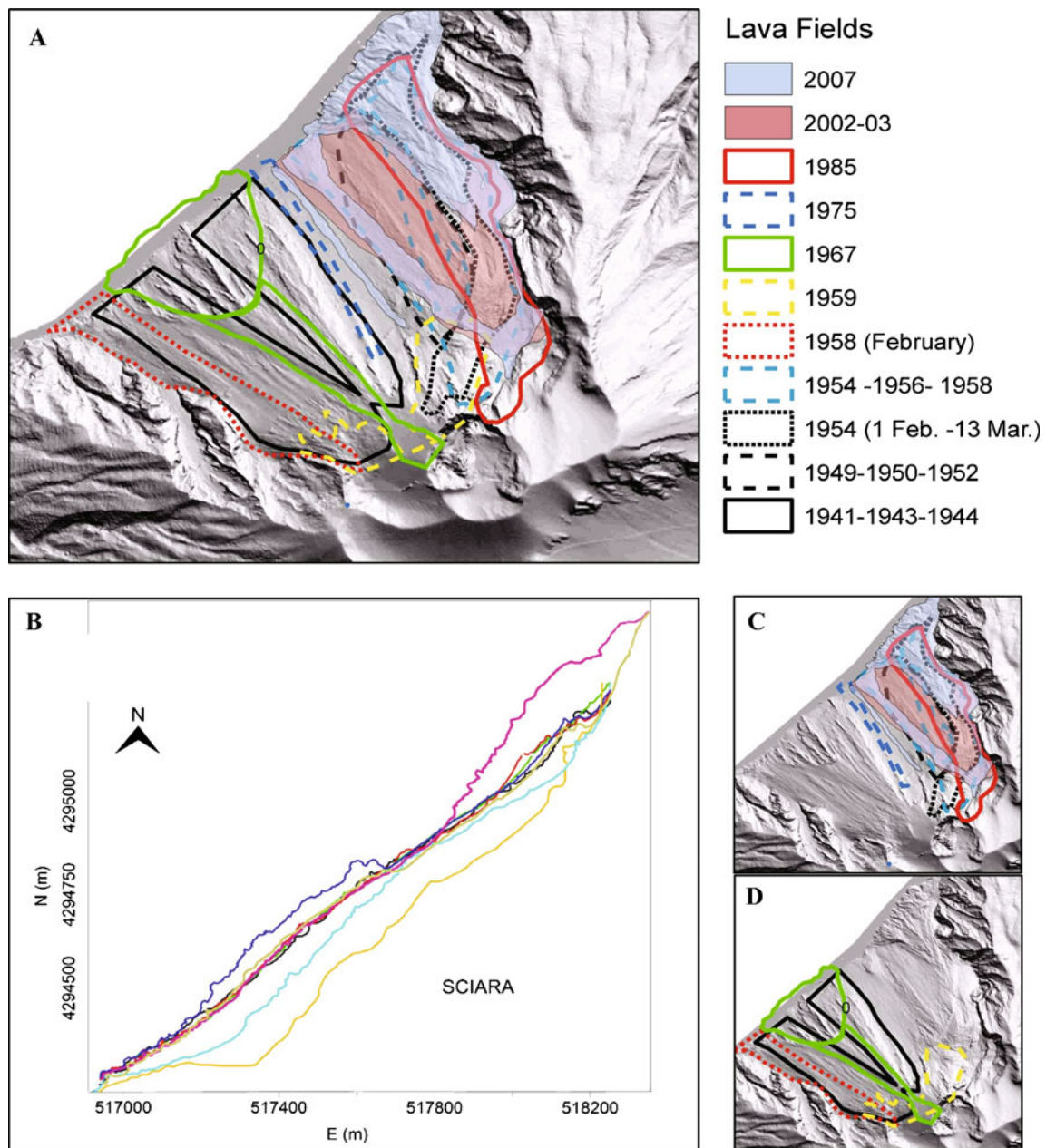


Fig. 8 Overall view of the reconstructed lava flows attributed to the different eruptions in the period 1937–2007: **a** overlapped lava fields on the whole slope, **b** evolution of the coastlines, **c** flows spreading along the SW side, **d** flows spreading along the NE side

the magnitude of the peak value of the effusion rate, the flow is able to reach the sea to form a lava delta. During the last two eruptions, we have eye-witnessed how the dike intrusion mechanism can trigger quite important instability phenomena that influence the lava flow discharge, as observed in 2007 when the lower vents appear positioned accordingly to structural discontinuities. Also, the flows were emplaced on a modified topography, as for instance in 2002–2003, when the lava filled the landslide scar instead of constructing a lava delta (Marsella et al. 2009). Finally, since in the considered period instability phenomena are not reported, we may infer that the north-eastern side of the

slope was gradually weakened by subsequent major eruptions, and now, it represents a preferential path for new lava intrusion from the deeper source.

Conversely, most of the eruptions that affected the south-western side (Fig. 8d) are characterized by lava flows of modest thicknesses and lava fields spread along the slope that usually do not reach the sea. This behaviour may be of course the consequence of lower effusion rate, but it also indicates that these eruptions may have been prevalently guided by overflow mechanisms from the eruptive vents located in the crater terrace rather than by dike intrusions.

Remarkably, the 1955 and the 1967 eruptions strongly differ from the others as most of the lava was emitted from a vent positioned at a lower altitude. This is certain for the 1967 eruption, for which we estimated that more than 80% of the lava was emitted from the lower vent at about 270 m a.s.l. However, using the available data, it was not possible to identify and quantify the 1955 eruption because the emission is reported to have been mainly underwater and also the possible traces were then completely covered by the 1967 flow. The 1955 vent opening at such low elevation can be explained by a lateral intrusion of magma from a deeper part of the plumbing system and not as the expression of an ephemeral vent of a higher fissure. In this respect, the existence of a structural weakness can be envisaged by considering that the morphological features observed in 1937 (the scar s in Fig. 4) and in 1967 (an eruptive fissure can be envisaged on the crater rim considering that the lava field depicted in Fig. 5d) appears aligned with the location of 1955 vent (Fig. 5d). Magma intrusions along this possible discontinuity have not occurred since the 1967 eruption.

The data listed in Table 4 are graphically summarized in Fig. 9a, highlighting the most relevant effusive episodes and their distribution all along the considered observation period. In addition the graph in Fig. 9b shows that the rate of the cumulative volume of erupted lava between 1937 and

1959 is higher (about $2 \text{ m}^3 \text{ s}^{-1}$) than that of the following period, even though the 1955 eruption and the submarine portion of the 1954 are not included. In the period 1960–2002, the activity is characterized by spaced out episodes showing an average eruption rate one order of magnitude lower ($0.2 \text{ m}^3 \text{ s}^{-1}$). In this period, the 1967 event represents the last large eruption emplaced along the south-western side the slope (even though its volume is underestimated). Finally, the last two eruptions may foretell the beginning of a more active period also characterized by a boost in the average discharge rate trend.

The analysis of the trend of the cumulative volume related to the lava flows can be considered significant for the assessment of Stromboli eruptive activity, even though it was not possible to include the volumes of the explosive products. Typical strombolian activity is quite regular and persistent, producing very low volumes of pyroclastic materials that mostly accumulate inside and in proximity of the crater terrace. Although reliable estimation of the past output rates it is quite difficult, an attempt to quantify the contribution of the volume of pyroclastic deposits was made by comparing two DEMs of the summit area acquired in 2004 and 2006. Since no lava flows or paroxysmal episodes were recorded in this period, the obtained average value of about $0.01 \text{ m}^3 \text{ s}^{-1}$ can be used as an indication to

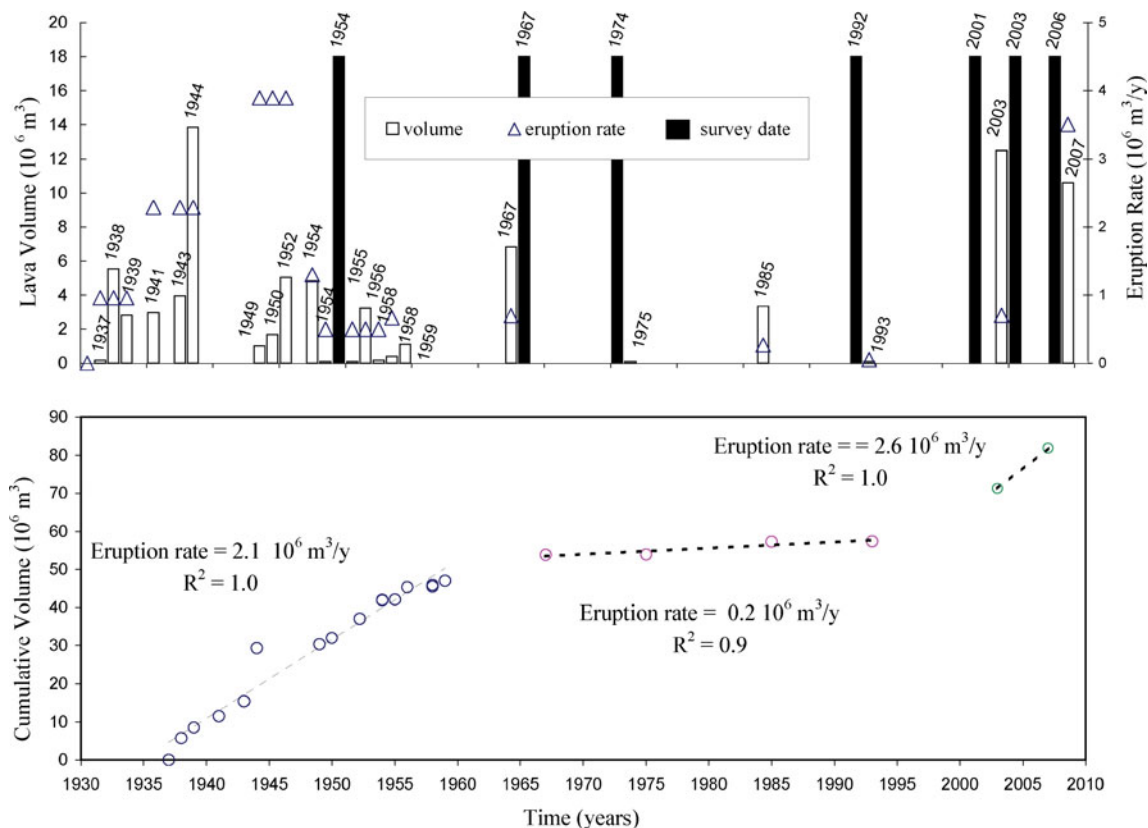


Fig. 9 Graphs of **a** the estimated erupted volume and eruption rate for the analysed events and **b** cumulative volume trend

evaluate the contribution for standard strombolian activity. Therefore, the trends illustrated in Fig. 9b should not be affected significantly by the variation of the low-energy explosive activity as well as by paroxysms since these occurred mainly in the period already characterized by higher eruption rates (1937–1959 and 2003–2007).

Conclusions

The conducted analysis permitted verification and integration of existing knowledge on Stromboli's recent effusive activity and, despite uncertainties due to the large observation time interval, represents a useful contribution for understanding and evaluating the hazards connected to lava flows that can induce instability of the steep Sciara del Fuoco slope.

Using a multi-temporal topographic dataset, extracted from historical maps, aerial photogrammetric and Airborne Laser Scanner surveys, we performed a quantitative reconstruction of the morphological changes of the Sciara del Fuoco on Stromboli Island between 1868 and 2009 inferring some key elements of the discharge mechanism characterizing the major eruptions at Stromboli. The main outcomes are the differentiation of distinctive eruptive styles in different sectors of the Sciara del Fuoco and to the identification of substantial differences in Stromboli's activity over the period of observation. Particularly, the effusive activity was very important, both in frequency and magnitude, in the first half of the century with respect to the following period, whereas the last two lava flow eruptions foresee a growth in the volumetric output rate. This should be considered a crucial aspect for the assessment of future effusive activity at Stromboli volcano.

Acknowledgements We are grateful to Alberico Sonnessa, Cristina Proietti and Silvia Scifoni who thoughtfully assisted in the development of the GIS project used for processing and mapping the topographic data. We thanks Benjamin van Wyk de Vries for thorough reviews which have improved the manuscript. This research was developed in the frame of the Project V1_2 coordinated by the 2004–2006 Department of Civil Protection and National Institute of Geophysics and Volcanology Research Program.

References

- Abruzzese D (1935) Attività dello Stromboli dal 1930 al 1934. *Boll Sism It* 33:118–121
- Abruzzese D (1937) Attività dello Stromboli dal 1934 al 1936. *Bull Volcanol* 11:205–210
- Abruzzese D (1940) Attività dello Stromboli dal 1937 al giugno 1939. *Bull Volcanol* 7:57–66
- Abruzzese D, Cavallaro C (1955) L'eruzione sottomarina dello Stromboli del 28 febbraio 1955. *Rivista "Stromboli" Messina* 5:25–29
- Baldi P, Fabris M, Marsella M, Monticelli R (2005) Monitoring the morphological evolution of the Sciara del Fuoco during the 2002–2003 Stromboli eruption using multi-temporal photogrammetry. *ISPRS J Photogramm Remote Sens* 59:199–211
- Baldi P, Bosman A, Chiocci FL, Marsella M, Romagnoli C, Sonnessa A (2008) Integrated sub-aerial- submarine evolution of the Sciara del Fuoco after the 2002 landslide. In: Calvari S et al (eds) *The Stromboli Volcano: An Integrated Study of the 2002–2003 Eruption Geophysical Monograph Series*, 182. AGU, Washington DC, pp 171–182
- Barberi F, Rosi M, Sodi A (1993) Volcanic hazard assessment at Stromboli based on review of historical data. *Acta Vulc* 3:173–187
- Bergevin R, Soucy M, Gagnon H, Laurendeau D (1996) Towards a general multi-view registration technique. *IEEE Trans Pat Anal Mach Intel* 18:540–547
- Besl PJ, McKay ND (1992) A methods for registration of 3D shapes. *IEEE Trans Pat Anal Mach Intel* 14:239–256
- Bullard FM (1954) Activity of Stromboli in June and December 1952. *Bull Volcanol* 15:91–98
- Capaldi G, Guerra I, Lo Bascio A, Luongo G, Pace R, Rapolla A, Scarpa R, Del Pezzo E, Martini M, Ghiara R, Lirer L, Munno R, La Volpe L (1978) Stromboli and its 1975 eruption. *Bull Volcanol* 41:1–27
- Cavallaro C (1957a) L'attività dello Stromboli dal 1940 al 1953. *Bollettino delle Seduta Accademia Gioenia Scienze Scienze Naturali Catania, Serie IV, Vol III, Fasc 10:1–6*
- Cavallaro C (1957b) L'attività dello Stromboli dall'aprile 1954 al 31 dicembre 1956. *Bollettino delle Seduta della Accademia Gioenia Scienze Scienze Naturali, Catania, Serie IV 3:103–118*
- Cavallaro C (1958) Un ciclo effusivo dello Stromboli (1–14 gennaio 1956; 16 gennaio–16 marzo 1956). *Atti della Società Peloritana di Scienze Fisiche Matematiche e Naturali Messina* 4:385–399
- Cavallaro C (1970) Le attività dello Stromboli nel triennio 1957–59 e le variazioni morfologiche da esse determinate. *Atti del XX Congresso Geografico Italiano (1967) pp 229–243*
- Cucuzza Silvestri S (1955) La recente attività dello Stromboli (febbraio-marzo 1954). *Bollettino delle Seduta Accademia Gioenia Scienze Naturali Catania, Serie IV 3:26–32*
- De Fino M, La Volpe L, Falsaperla S, Frazzetta G, Neri G, Francalanci L, Rosi M, Sbrana A (1988) The Stromboli eruption of December 6, 1985–April 25, 1986: volcanological, petrological and seismological data. *Rend Soc It Miner e Petr* 43:1021–1038
- Gasparini P, Lirer L, Luongo G (1968) Caratteristiche petrochimiche e fisiche della lava emessa dallo Stromboli nell'aprile del 1967. *Ann Osserv Vesuv* 8:13–18
- Gruen A, Akca D (2005) Least square 3D surface and curve matching. *ISPRS J Photogramm Remote Sens* 59:151–174
- Gruner H (1977) *Photogrammetry:1776–1976*. Photogramm Eng Remote Sens 43:569–574
- Imbo' G (1933) Parossismo di Stromboli del Settembre 1930. *Bull Volcanol* 15:177–185
- Kokelaar P, Romagnoli C (1995) Sector collapse, sedimentation and clast population evolution at an active island-arc volcano – Stromboli, Italy. *Bull Volcanol* 57:240–262
- Kraus K (1998) *Photogrammetry*. Dümmler, Bonn
- Maas HG (2003) Planimetric and height accuracy of a Airborne Laser Scanner data - User requirements and system performance. In: Fritsch D (ed) *Proc n 49 Photogrammetric Week*. Wichmann, Germany, pp 117–125
- Magnani M (1939) Osservazioni geologiche e morfologiche sull'isola di Stromboli. *L'Universo* 11:837–869
- Marsella M, Coltelli M, Proietti C, Branca S, Monticelli R (2008) 2002–2003 Lava flow eruption of Stromboli in a contribution to understanding lava discharge mechanism using periodic digital

- photogrammetric surveys. In: Calvari S et al (eds) *The Stromboli volcano: an integrated study of the 2002–2003 eruption*. AGU, Washington DC, pp 229–246
- Marsella M, Sonnessa A, Proietti C, Bernardo E, Coltelli M, Tommasi P (2009) The evolution of the Sciara del Fuoco sub-aerial slope during the 2007 Stromboli eruption: relation between deformation processes and effusive activity. *J Volcanol Geotherm Res*. doi:101016/jjvolgeores200902002
- Nappi G (1976) L'eruzione dello Stromboli bel Novembre 1975. *Boll Soc Geol It* 95:991–1008
- Pasquaré G, Francalanci L, Garduño VH, Tibaldi A (1993) Structure and geologic evolution of the Stromboli volcano. *Aeolian Islands, Italy Acta Vulcanol* 3:79–89
- Pilgrim LJ (1996) Surface matching and difference detection without the aid of control points. *Surv Rev* 33:291–304
- Ponte G (1948) Attività straordinaria dello Stromboli. *Ann Geofis* 1:200–202
- Proietti C, Coltelli M, Marsella M, Sonnessa A, Bernardo E (2008) Photogrammetric and LIDAR surveys on the Sciara del Fuoco to monitor the 2007 Stromboli eruption. In *Proc USEReST 2008*, Napoli doi:101109/USEREST20084740348
- Rittmann A (1931) Der Ausbruch des Stromboli am 11 September 1930. *Zeits f Vulkanol* 14:47–77
- Rosi M, Bertagnini A, Landi P (2000) Onset of the persistent activity at Stromboli Volcano (Italy). *Bull Volcanol* 62:294–300
- Tibaldi A (2001) Multiple sector collapses at Stromboli volcano, Italy: how they work. *Bull Volcanol* 63:112–125
- Tinti S, Manucci A, Pagnoni G, Armigliato A, Zaniboni F (2005) The 30 December 2002 landslide-induced tsunamis in Stromboli: sequence of events reconstructed from the eyewitness accounts. *Nat Hazards Earth Syst Sci* 5:763–775
- Tommasi P, Baldi P, Chiocci FL, Coltelli M, Marsella M, Pompilio M, Romagnoli C (2005) The landslide sequence induced by the 2002 eruption at Stromboli volcano. In: Sassa K, Fukuoka H, Wang FW, Wang G (eds) *Landslide—risk analysis and sustainable disaster management*. Springer, New York, pp 251–258
- Tommasi P, Baldi P, Chiocci FL, Coltelli M, Marsella M, Romagnoli C (2008) Slope Failures Induced By The December 2002 Eruption At Stromboli Volcano. In: Calvari S et al (eds) *The Stromboli Volcano: An Integrated Study of the 2002–2003 Eruption*. Geophysical Monograph Series vol 182. AGU, Washington DC, pp 229–246